Chapter 6

Stability Enhancement of Dye-Sensitized Solar Cells Fabricated with Gel Electrolyte

This page is intentionally left blank

6.1. Introduction

Due to continuously increasing energy demand, the polluting environment, and the rising price of fossil fuels, scientists are constantly thinking of new ways to find pollution-free renewable energy sources [1]. The natural resources that can renew themselves over time are called renewable energy sources [2]. It is believed that solar energy would be the main source of alternative energy [3]. Conventional Crystalline and polycrystalline silicon solar cells have attained energy conversion efficiency of over 20%, but due to their complicated and difficult fabrication process and high cost [4], people have started to think about its alternative. Grätzel and co-workers first reported DSSCs as a useful substitute for conventional solar cells [1], and subsequently, a considerable interest has been developed in DSSCs because of their easy fabrication technique and low cost [5].

Photo anode of a DSSC performs a vital role in determining the overall performance of the DSSC by transporting electrons and supporting the Dye molecules [7, 8]. The semiconducting oxide material TiO_2 is mostly used as a photoanode because of its excellent optical, electrical, and chemical properties [9-12]. Although appreciably high conversion efficiency is achieved with TiO_2, its low electron mobility results in low electron mobility have led to renewed investigations into new alternative wide-bandgap photoanode materials like ZnO, WO_3, and SnO_2 for better performance of Dye-sensitized solar cells [13-15]. Researchers are also using natural dyes extracted from different fruits, vegetables, and flowers in search of low-cost DSSC fabricated with environment-friendly and non-toxic material [16-20].

But the electrolyte has a close interaction with all the components of DSSC and it determines the time stability of the cell. Due to this, scientists have been paying more attention to electrolytes these days [21, 22]. Though the theoretically estimated maximum photoelectric conversion efficiency of a DSSC is 29 % [23] has been recorded with liquid electrolytes, the actual

efficiency of 14.3% could be achieved. This is due to leakage problems of liquid electrolytes, electrode corrosion, photo-degradation of attached dyes, and solvent volatility restricts the long-term performance of DSSCs [24]. To overcome these limitations, gel electrolytes have been used instead of liquid electrolytes as the volatility of organic solvents can be decreased and leakage can be prevented by gel-type electrolytes [25]. Gel electrolytes are usually prepared by adding materials of high molecular weights with organic solvents and iodides. Polyvinyl carbonate (PC), Acetonitrile (ACN), and ethylene carbonate (EC) are an example of some of the popularly used solvents and Lithium iodide (LiI), potassium iodide (KI), Sodium iodide are some of the commonly utilized iodides with iodine (I_2). For gelation of liquid electrolytes, many materials are used, namely polyethylene glycol, polyvinylidene fluoride-co-hexafluoropropylene (PVDF-HFP), polyethylene oxide, etc. [26].

In this study, we prepared gel electrolytes using ethyl cellulose (EC) as a gelator in the liquid electrolyte and fabricated DSSCs with both liquid and gel electrolytes to study to study their overall photovoltaic performance, including their performance stability over a certain period. We used both TiO_2 and ZnO as working electrode material. The effect of EC concentration on the performance of DSSCs was also examined. A detailed comparison of photoelectric properties of all the cells is presented in the investigation.

6.2. Materials and Methods

6.2.1 Materials

All the chemicals used in this study were purchased from commercial sources and used as received. Fluorine-doped tin oxide (FTO) glass slides (10 Ω/square; thickness 2.2 mm), ruthenium dye (N3 and N719), Surlyn spacer, and Platinum Precursors solution (Plastisol T) for counter electrode preparation, all were purchased from Solaronix, Switzerland. Titanium dioxide nanopowder (TiO_2), ZnO nanopowder, Lithium Iodide (LiI), and Iodine (I_2)

were purchased from Sigma-Aldrich, India. The chemicals, used in gel preparation are Acetonitrile (Merck, India), 4-tert-butylpyridine (TCI CHEMICALS, Japan), Tetrabutylammonium iodide (Merck), Ethyl Cellulose (Sigma-Aldrich, India), acetone (C_3H_6O), ethanol (C_2H_5OH), and acetic acid (CH_3CO_2H) (Sigma-Aldrich, India). All the reagents purchased were of analytical grade and were used without further purification.

6.2.2 Preparation of liquid and gel electrolyte

The liquid electrolyte, used in this study, was prepared by mixing LiI (0.5M) and I_2 (0.05M) in 10 ml acetonitrile solvent. To prepare the gel electrolyte, ethyl-cellulose powder mixed with ethanol was added to the prepared liquid electrolyte at different amounts to yield gel electrolyte of concentrations of 2, 4, 6, 8 and 10 wt%. Fig.6.1 represents different steps of electrolyte preparation.

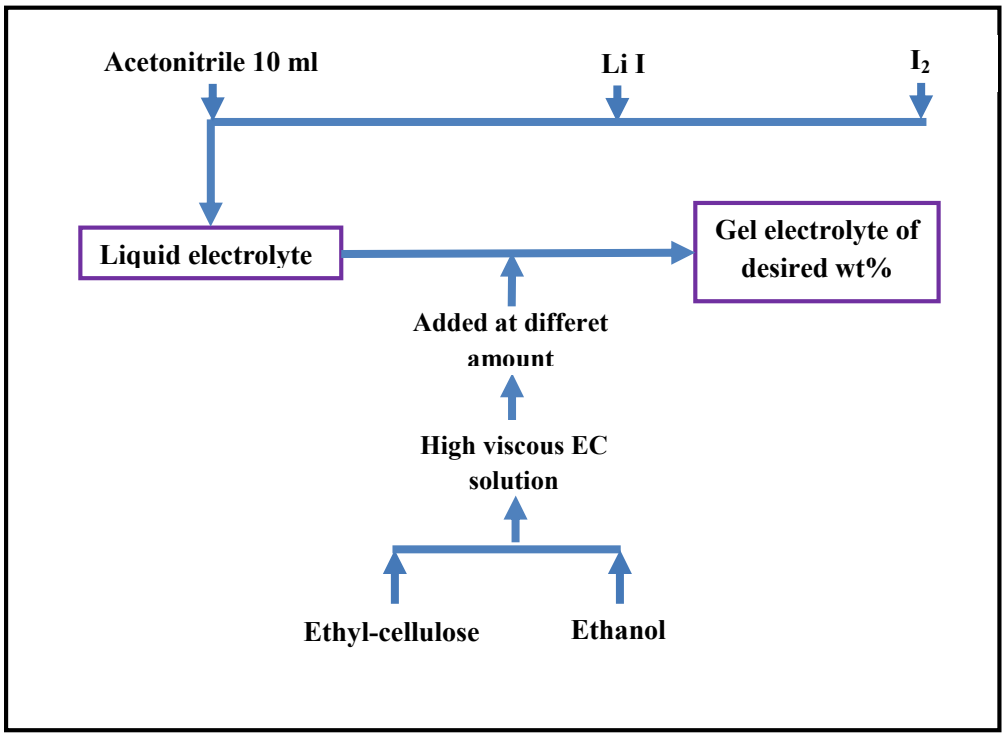

Figure 6.1 Steps of Liquid and Gel electrolyte preparation.

6.2.3 Fabrication of the solar cells

The TiO_2 and ZnO working electrodes of the DSSC were prepared by following the standard procedure [27]. At first, 10 gm of the nanopowder was mixed with diluted acetic (1ml in 50 ml deionized water) acid in a mortar and pastel and added a few drops of Triton X100 (Merck) as surfactant and ground continuously until a homogenous, smooth suspension was obtained. The lump-free slurry was then applied on the conductive side of an FTO-coated glass using the doctor blade method to make a homogeneous layer. To strengthen the bonding between the FTO glass and the semiconductor paste, the nanopowder coated FTO glass plates were sintered in normal atmospheric condition at 450°C for 45 minutes. In the sintering process, after introducing the sample in the furnace, the temperature was raised with a rate of 10°C/5 min until the temperature had reached 350°C and after that, it was increased with a rate of 10°C/10 min until 450°C. When it cooled down to room temperature, the sintered substrates were immersed in the ruthenium dye (N3) solution for dye adsorption on the surface of the TiO_2 and ZnO nanoparticles for 24 hours. FTO glass coated with a platinum catalyst (Plastisol-T) and heated at 400°C was used as a counter electrode and a sealed sandwich-type cell was fabricated by assembling dye adsorbed working electrode and the platinum (Pt) coated counter electrode with Surlyn film as a spacer between them. The electrolyte was introduced into the assembled cell through a pre-drilled hole on the counter with a syringe. Gel electrolyte having different EC concentration was used in different cells for the investigation. A small piece of Surlyn spacer and glass glue was used to seal the hole and finally, the cells were connected to the external circuit with the help of alligator clips. Different electrolyte concentrations were used to fill the cells.

6.2.4 Characterization of the DSSCs

After completing the fabrication of two different cells with liquid and gel type electrolytes, the cells were placed under artificial solar illumination of 100mW/cm^2 and connected with the J-V measurement system to calculate the photoelectric conversion efficiencies [28]. The photocurrent voltage (J-V) characteristics were recorded using a Keithley 2400 source meter. Simulated sunlight was supplied using a xenon lamp (450W). The photovoltaic performances were recorded at a 24 hr interval to investigate the long-term stability of the DSSCs. The ethyl cellulose as gelator was selected for its easy availability and low cost. Symmetrical cells having Pt-electrolyte-Pt structure were configured to perform the EIS measurement of the electrolyte system. Pt electrodes were prepared by coating the FTO substrate using the same Pt catalyst solution as used in conventional DSSCs.

6.3 Results and Discussions

6.3.1 Raman spectroscopy of TiO_2 and ZnO

Fig. 6.2 shows the Raman spectra of TiO_2 and ZnO nanopowders. The Raman shifts of Fig. 6.2 (a) at 235, 447, and 612 cm^{-1} are attributed to the combination of two-phonon scattering modes, E_g and A_{1g} modes of the rutile phase, respectively[29, 30]. According to the literature values, all the observed spectroscopic peaks listed in Fig. 6.2 (b) can be assigned to a wurzite ZnO structure. Among these Raman peaks, the E_2 mode centred at 437 cm^{-1} has a strongerintensity and narrower line-width, which indicates that the as-grown products are composed of ZnO with a hexagonal wurtzite structure and good crystal quality [31].

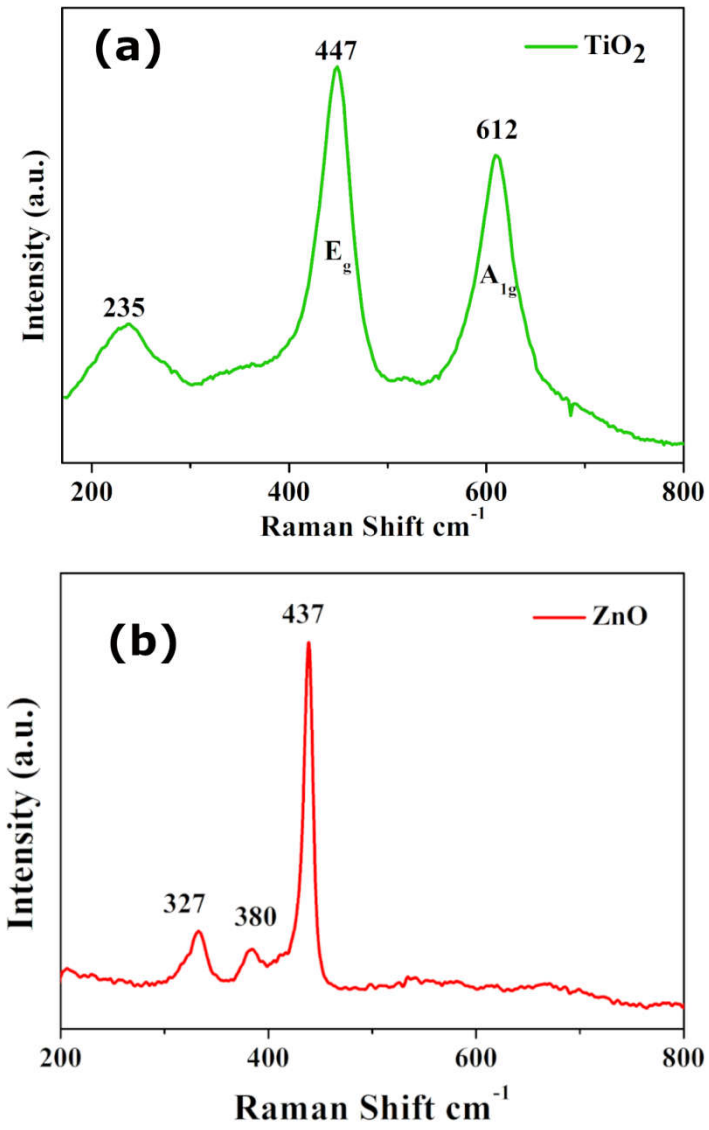

Figure 6.2 Raman spectra of (a) TiO_2 and (b) ZnO nanoparticles**.**

6.3.2 Scanning electron microscope (SEM) analysis

The scanning electron microscope (SEM) was used to examine the surface morphology of the photoanode films over the FTO glass substrate [29]. The highly porous morphology of the TiO_2 and ZnO nanostructure films deposited on the FTO glass substrate can be observed from the SEM images shown in Fig. 6.3(a) and Fig. 6.3(b) respectively.

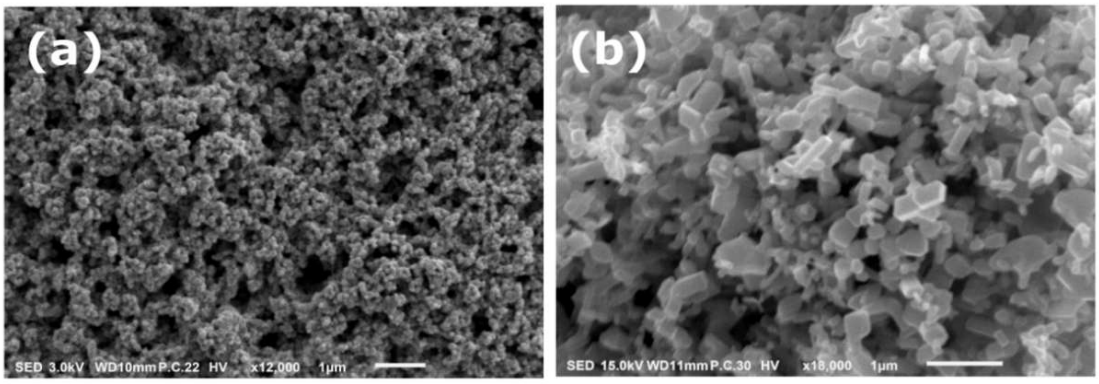

Figure 6.3 Scanning electron microscope (SEM) image of (a) TiO_2 and (b) ZnO nanoparticles**.**

The average particle size of the TiO_2 nanoparticles was about 20 nm while that was in a range of 40-300 nm for ZnO. The highly porous structure of the semiconductor thin film resulted in greater dye molecule adsorption on the surface of the TiO_2 and ZnO nanoparticles. Also, the smaller particle size of the TiO_2 nanoparticles compared to ZnO provides a higher overall surface area for dye molecule attachment for a particular volume of the photoanode. More dye adsorption causes more electron excitation from HOMO to LUMO of dye molecules after photon absorption [32].

6.3.3 Photovoltaic Performance of the DSSCs

The Current-Voltage (I-V) characteristics of the N719 dye and TiO_2 photoanode based DSSCs fabricated using liquid and gel-based electrolytes are shown in Fig. 6.4.

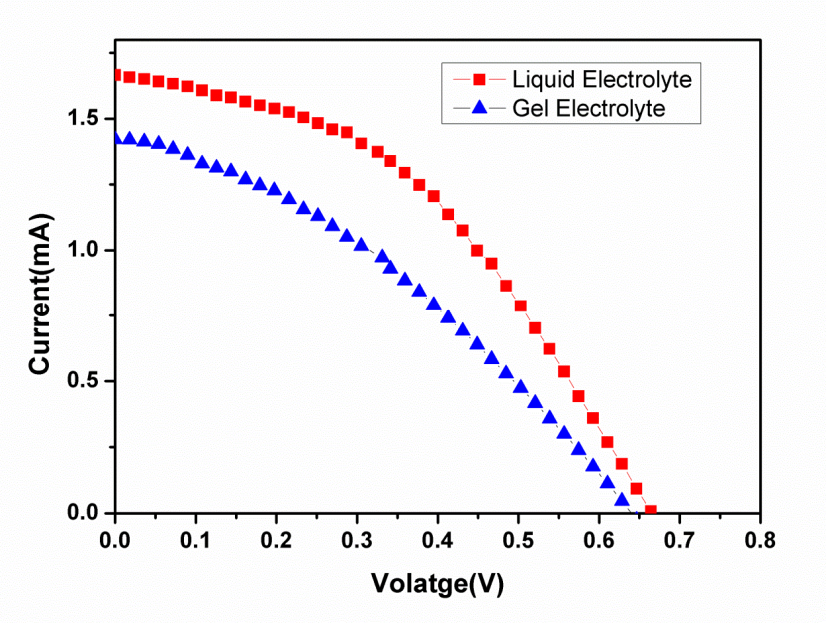

Figure 6.4 Current-Voltage characteristics of the N719 dye based cells fabricated with TiO_2.

The different electrical parameters of the cells obtained from the I-V characteristics are listed in Table 6.1 below.

Table 6.1. Summary of photovoltaic parameters of the N719 dye based cells.

Electrolyte used	J_{sc} (mA/cm^2)	V_{oc}(V)	FF	Efficiency (η %)
Liquid	1.67	0.662	0.43	1.90
Gel	1.42	0.646	0.35	1.29

The energy conversion efficiency of gel electrolyte based DSSC was lower than liquid electrolyte based DSSC. The photovoltaic efficiency of DSSCs using liquid and gel type electrolytes is 1.90% and 1.29% respectively. Table 6.1 represents the various photovoltaic parameters extracted from the I-V curves of the cells with liquid and gel electrolytes. The solar cell fabricated using liquid electrolyte exhibits higher short-circuit photocurrent density (J_{SC}),

open-circuit voltage (V_{OC}), and fill factor (FF) compared to the DSSC fabricated using gel electrolyte as a dye.

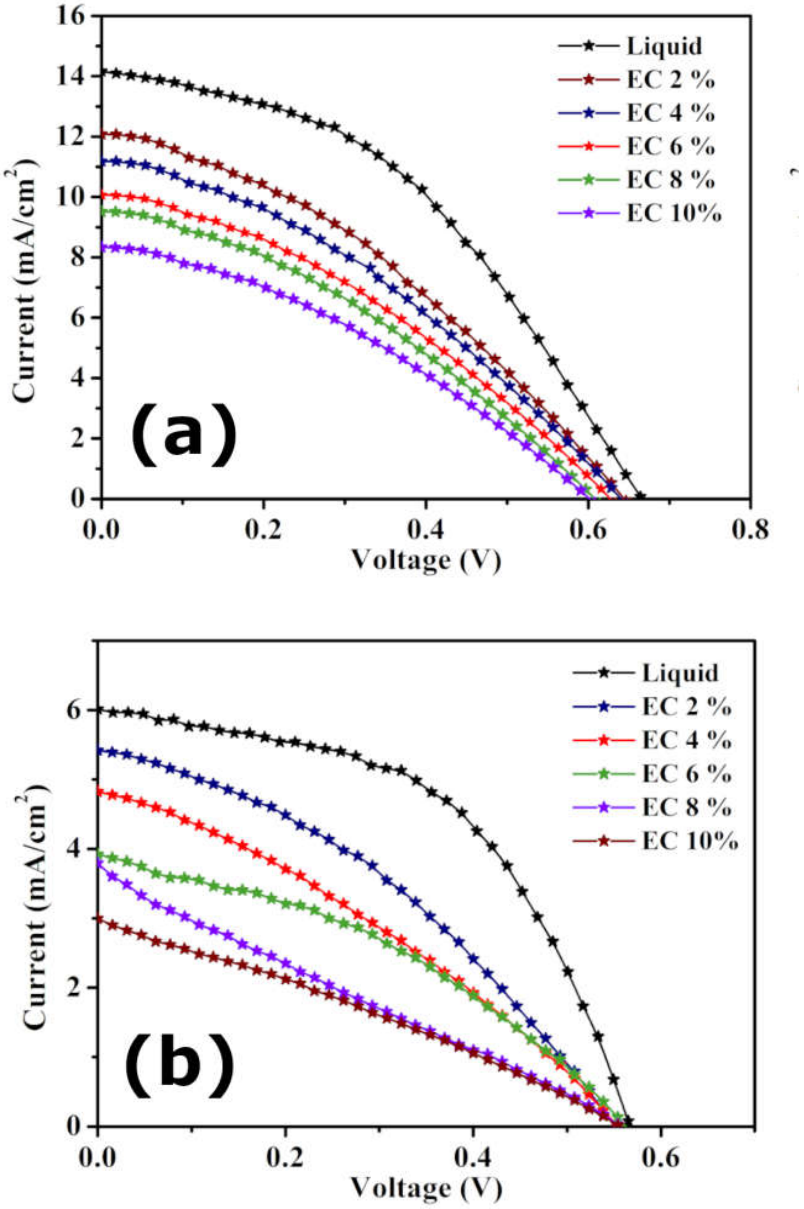

Figure 6.5 Current-Voltage characteristics of the N3 dye based cells fabricated with (a) TiO_2 (b) ZnO photoanodes.

The Current-Voltage (I-V) characteristics of the DSSCs fabricated using liquid and gel-based electrolytes are shown in Fig. 6.5. The different electrical arameters of the cells obtained from the I-V characteristics are listed in Table 6.2 below.

Table 6.2. Summary of photovoltaic parameters of the N3 dye based cells.

Cell	wt% of EC	J_{sc} (mA/cm^2)	V_{oc}(V)	FF	Efficiency (η %)
TiO_2	0	14.16	0.66	0.43	4.01
	2	12.0	0.64	0.37	2.84
	4	11.18	0.64	0.35	2.50
	6	10.06	0.63	0.34	2.15
	8	9.51	0.61	0.34	1.97
	10	8.33	0.60	0.34	1.70
ZnO	0	6.01	0.56	0.51	1.71
	2	5.41	0.55	0.36	1.07
	4	4.82	0.55	0.32	0.85
	6	3.91	0.56	0.36	0.79
	8	3.79	0.55	0.24	0.50
	10	2.99	0.55	0.28	0.46

It can be seen from Fig. 6.5(a) and 6.5(b) that for both TiO_2 and ZnO photoanode based DSSCs, there is a loss of device performance with an increase in EC content. This is due to increased electrolyte viscosity and decreased ionic diffusion coefficient with an increase in EC amount. The energy conversion efficiency of gel electrolyte based DSSCs was much lower than the liquid electrolyte based DSSCs in both TiO_2 and ZnO photoanode based cells. The photovoltaic efficiency of DSSCs using liquid and gel type electrolytes is 4.01 % and 2.84 % respectively for TiO_2 based cells, and

for ZnO based cells, these values are 1.71 % and 1.10 % respectively. Table 6.2 represents the various photovoltaic parameters extracted from the I-V curves of the cells with liquid and gel electrolytes. The efficiency of the gel-based DSSC for both the N719 and N3 dye may be low compared to the liquid electrolyte based DSSC, but the values of cell parameters obtained are found to be comparable to the efficiencies obtained for gel electrolyte based DSSCs [32]. For both TiO_2 and ZnO photoanodes, we had the highest efficiency in gel-based cells for 2 wt% EC concentration. The TiO_2 based devices showed better performance as compared to ZnO based devices which were quite expected.

6.3.4 Electrochemical behavior analysis of the DSSCs

Electrochemical Impedance Spectroscopy (EIS) is a very useful technique for interpreting the kinetics of charge transport processes in different layers of DSSCs [33]. To quantify the effect of EC content on the diffusion property of the electrolyte, EIS measurement was employed in Pt-electrolyte-Pt cells with an electrolyte having various content of EC in the liquid electrolyte and the obtained Nyquist plot is shown in Fig. 6.6. Generally the Nyquist plot of a Pt-electrolyte-Pt cell consists of two semicircles. First semicircle corresponding to high-frequency range represents the charge transfer resistance in the Pt-electrolyte interface, and the second semicircle in the low-frequency range represents Warburg diffusion element due to diffusion of iodide / tri-iodide ion in the electrolyte. An equivalent circuit shown in the inset of Fig. 6.4 is incorporated to analyze the EIS data. R_s corresponds to the series resistance of the electrical contacts and the FTO substrate present in the cell, R_{Pt} represents the resistance in the Pt counter electrode/electrolyte interface and C_{pt} represents corresponding capacitance. W represents impedance (corresponding resistance is R_w) due to the Warburg diffusion process of I^-/I_3^- in the electrolyte [22, 33-36].

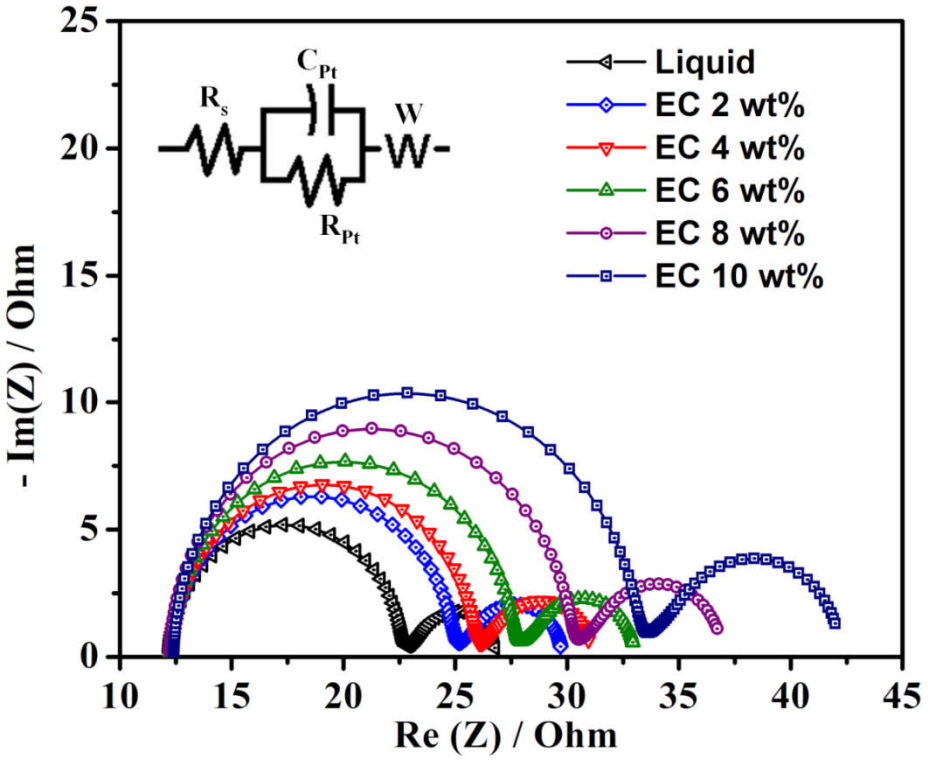

Figure 6.6 Nyquist plot of the Pt-electrolyte-pt cells with liquid and gel electrolyte with different EC content.

Different parameters extracted from Fig. 6.6 by fitting with the equivalent circuit are summarised in Table 6.3. The variations in R_{Pt} and R_w are caused by the differences in conductivities in the relevant electrolytes. It can be seen that both R_{pt} and R_w is the lowest for liquid electrolyte, indicating the highest conductivity of the electrolyte [37]. Increased values of R_{pt} and R_w with increase in EC content indicates deceased conductivity and hence decreased cell performance which is in well agreement with the current-voltage measurement of both TiO_2 and ZnO cells given in Table 6.2. Increased values of diffusion resistance (R_w) with increased EC content implies decreased diffusion rate of I^- and I_3^- ions in the electrolyte and thereby slightly lowering the J_{sc} and η with an expected increase in device stability by preventing leakage of electrolyte. It also suggests that the more viscous gel electrolyte does not

affect the charge transfer process very much for EC concentration of 2 Wt% in the photoanode/electrolyte interface of the cell as compared to the liquid electrolyte.

Table 6.3. EIS measurement results of the Pt-Electrolyte-Pt cells with liquid electrolyte and gel electrolyte having different EC content.

EC Concentration	$R_s(\Omega)$	$R_{Pt}(\Omega)$	$R_w(\Omega)$
0 Wt% (Liquid)	12.25	10.30	4.25
2 Wt%	12.30	12.52	4.93
4 Wt%	12.32	13.46	5.27
6 Wt%	12.28	15.25	5.48
8 Wt%	12.25	17.83	6.85
10 Wt%	12.41	20.58	9.23

6.3.5 Stability Study of the Cells

To explore the effect of electrolytes on long-term stability, the DSSCs were characterized by performing photovoltaic measurement over time. The sealed cells were placed under 1 sun illumination and J-V measurements were recorded every day over fifteen days. The stability check was performed for both TiO_2 and ZnO DSSCs fabricated with liquid and gel electrolytes. The gel electrolyte with EC content of 2 wt% was only chosen for stability measurements and the cells with gel electrolytes having EC content of more than 2 wt% showed significantly decreased efficiency. Figure 6.7 depicts J_{sc} , V_{oc} , FF, and η over time for liquid DSSCs and gel DSSCs fabricated with both TiO_2 and ZnO as photoanode material.

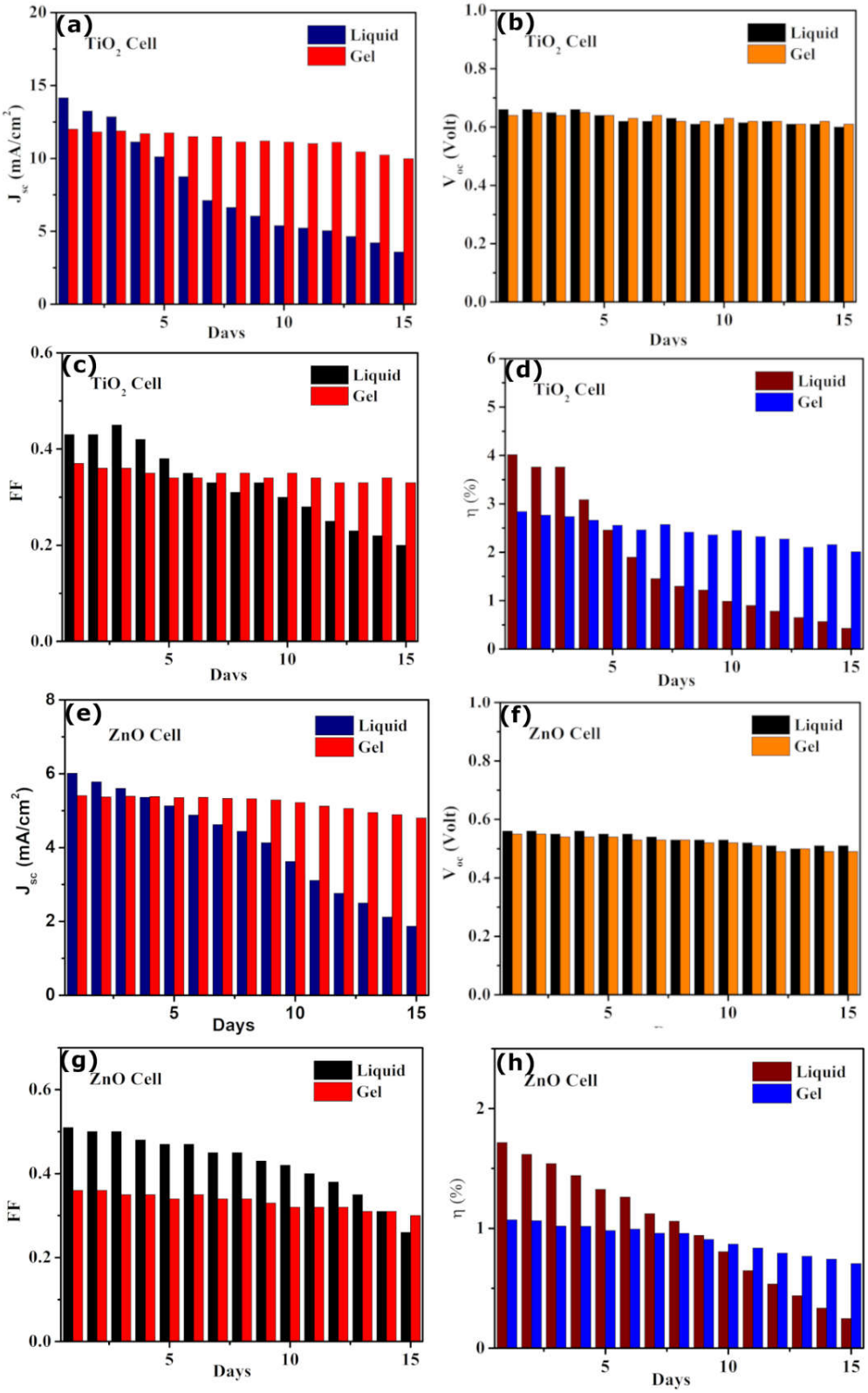

Figure 6.7 Stability behaviour of the liquid and gel based DSSCs fabricated with (a)-(d) TiO_2 and (e)-(h) ZnO as photoanode material.

It is clearly evident from Fig.675 that incorporating EC into the DSSC electrolyte improves device stability significantly for both types of DSSCs. V_{oc} remains almost unchanged for both liquid and gel electrolytes, whereas FF and J_{sc} decrease rapidly for liquid electrolyte-based DSSCs, but this decline is much slower for Gel electrolyte cells. Consequently, the efficiency of the gel electrolyte-based cells is well stable compared to the efficiency of liquid electrolyte-based cells, which decreases rapidly over time. It is clear that even though there is a slight decrease in the efficiency of the gel electrolytes, the cell developed with gel electrolytes shows better stability than that with liquid electrolyte. The improvement in long-term stability is probably due to the higher viscosity of gel, inhibiting the ionic migration to stabilize the system over a longer time and also by controlling the evaporation of liquid electrolytes [38]. Also, the higher stability of the gel electrolyte gives it better cost-effectiveness than the liquid electrolyte.

6.4 CONCLUSION

DSSCs were fabricated with pure TiO_2 and ZnO photoanodes with liquid and gel-type electrolyte, and cell performances were recorded. The liquid electrolyte cells exhibited higher short-circuit photocurrent density, open-circuit voltage, fill factor, and efficiency compared to the gel electrolyte based DSSCs. Though the efficiency of the gel-based DSSC is lower than the liquid electrolyte DSSC, the cell parameters obtained were comparable to the parameters obtained for gel electrolyte DSSCs by other researchers. Comparing these two types of DSSCs, it is clear that though the photovoltaic performance of gel electrolyte DSSC is slightly lower than liquid electrolyte DSSC, the performance of gel-based DSSC remains noticeably stable while for the liquid electrolyte the stability decreases remarkably over time. It is also found that the EC based gel electrolyte with proper EC wt% can be used to increase the stability of both TiO_2 and ZnO photoanode based DSSCs.

References:

[1] Grätzel, M., "Dye-sensitized solar cells", *Journal of photochemistry and photobiology C: Photochemistry Reviews*, vol. 4, no. 2, pp. 145-153, 2003.
https://doi.org/10.1016/S1389-5567(03)00026-1

[2] Elliott, D., "Renewable energy and sustainable futures", *Futures*, vol. 32, no. 3-4, pp.261-274., 2000.
https://doi.org/10.1016/S0016-3287(99)00096-8

[3] Gong, J., Liang, J., Sumathy, K., "Review on dye-sensitized solar cells (DSSCs): fundamental concepts and novel materials", *Renewable and Sustainable Energy Reviews*, vol. 16, no. 8, pp. 5848-5860, 2012.
https://doi.org/10.1016/j.rser.2012.04.044

[4] Blakers, A., Zin, N., McIntosh, K. R., Fong, K., "High-efficiency silicon solar cells", *Energy Procedia*, vol. 33, pp. 1-10, 2013.
https://doi.org/10.1016/j.egypro.2013.05.033

[5] McConnell RD., "Assessment of the dye-sensitized solar cell. *Renewable and Sustainable Energy Reviews*", vol. 6, no. 3, pp. 271-93, 2002.
https://doi.org/10.1016/S1364-0321(01)00012-0

[6] Sharma K, Sharma V, Sharma SS, "Dye-sensitized solar cells: fundamentals and current status", *Nanoscale research letters*, vol. 13, no. 1, pp. 381, 2018.
https://doi.org/10.1186/s11671-018-2760-6

[7] Al-Alwani MA, Mohamad AB, Ludin NA, Kadhum AA, Sopian K., "Dye-sensitised solar cells: development, structure, operation principles, electron kinetics, characterization, synthesis materials & natural photosensitizers", *Renewable & Sustainable Energy Reviews*, vol. 65, no. 1, pp. 183-213, 2016.
https://doi.org/10.1016/j.rser.2016.06.045

[8] O'regan B, Grätzel M. A, "low-cost, high-efficiency solar cell based on dye-sensitized colloidal TiO2 films", *Nature*, vol. 353, no. 6346, pp. 737-740, 1991.
https://doi.org/10.1038/353737a0

[9] Leung DY, Fu X, Wang C, Ni M, Leung MK, Wang X, et al. "Hydrogen production over titania-based photocatalysts", *ChemSusChem*, vol. 3, no. 6, pp. 681-694, 2010.
https://doi.org/10.1002/cssc.201000014

[10] Liu G, Gong J, Kong L, Schaller RD, Hu Q, Liu Z, et al., "Isothermal pressure-derived metastable states in 2D hybrid perovskites showing enduring bandgap narrowing", *Proceedings of the National Academy of Sciences*, vol. 115, no. 32, pp. 8076-8081, 2018.
https://doi.org/10.1073/pnas.1809167115

[11] Liu G, Kong L, Guo P, Stoumpos CC, Hu Q, Liu Z, et al., "Two regimes of bandgap redshift and partial ambient retention in pressure-treated two-dimensional perovskites", *ACS Energy Letters*, vol. 2, no. 11, pp. 2518-2524, 2017.
https://doi.org/10.1021/acsenergylett.7b00807

[12] Wang X, Li Z, Shi J, Yu Y, "One-dimensional titanium dioxide nanomaterials: nanowires, nanorods, and nanobelts", *Chemical Reviews*, vol. 114, no. 19, pp. 9346-9384, 2014.
https://doi.org/10.1016/j.ijleo.2019.164142

[13] Biswas R, Chatterjee S, "Effect of surface modification via sol-gel spin coating of ZnO nanoparticles on the performance of WO_3 photoanode-based Dye-Sensitized Solar Cells", *Optik*, 2019 Dec 28:164142.
https://doi.org/10.1016/j.ijleo.2019.164142

[14] Lee JH, Park NG, Shin YJ, "Nano-grain SnO_2 electrodes for high conversion efficiency SnO_2–DSSC", *Solar energy materials and solar cell*, vol. 95, no. 1, pp. 179-183, 2011. https://doi.org/10.1016/j.solmat.2010.04.027

[15] Zheng H, Tachibana Y, Kalantar-Zadeh K, "Dye-sensitized solar cells based on WO_3", *Langmuir*, vol. 26, no. 24, pp. 19148-19152, 2010. https://doi.org/10.1021/la103692y

[16] Karki IB, Nakarmi JJ, Mandal PK, Chatterjee S, "Effect of organic dyes on the performance of ZnO based dye-sensitized solar cells", *Applied Solar Energy*, vol. 49, no. 1, pp. 40-45, 2013. https://doi.org/10.3103/S0003701X13010052

[17] Ayalew WA, Ayele DW, "Dye-sensitized solar cells using natural dye as light-harvesting materials extracted from Acanthus sennii chiovenda flower and Euphorbia cotinifolia leaf", *Journal of Science: Advanced materials and devices*, vol. 1, no. 4, pp. 488-494, 2016. https://doi.org/10.1016/j.jsamd.2016.10.003

[18] Kabir F, Bhuiyan MM, Manir MS, Rahaman MS, Khan MA, Ikegami T, "Development of dye-sensitized solar cell based on a combination of natural dyes extracted from Malabar spinach and red spinach", *Results in Physics*, vol. 14, no. 1, pp. 1-7, 2019. (Article no.102474) https://doi.org/10.1016/j.rinp.2019.102474

[19] Narayan MR, "Dye-sensitized solar cells based on natural photosensitizers", *Renewable and Sustainable Energy Reviews*, vol. 16, no. 1, pp. 208-215, 2012. https://doi.org/10.1016/j.rser.2011.07.148

[20] Biswas R, Roy T, Chatterjee S, "Study of Electro-Optical Performance and Interfacial Charge Transfer Dynamics of Dye-Sensitized Solar Cells Based on ZnO Nanostructures and Natural Dyes", *Journal of Nanoelectronics and Optoelectronics*, vol. 14, no. 1, pp. 99-108, 2019. https://doi.org/10.1166/jno.2019.2445

[21] Wu, J., Lan, Z., Hao, S., Li, P., Lin, J., Huang, M., et al., "Progress on the electrolytes for dye-sensitized solar cells", *Pure and Applied Chemistry*, vol. 80, no. 11, pp. 2241-2258, 2008. https://doi.org/10.1351/pac200880112241

[22] Vasei, M, Tajabadi, F., Jabbari, A. & Taghavinia, N., "Stable dye-sensitized solar cells based on a gel electrolyte with ethyl cellulose as the gelator", Applied Physics A volume 120, pages869–874(2015) https://doi.org/10.1007/s00339-015-9332-8

[23] Richter, A., Hermle, M., Glunz, S. W, "Reassessment of the limiting efficiency for crystalline silicon solar cells", *IEEE Journal of photovoltaics*, Vol. 3, no. 4, pp. 1184-1191, 2013. https://doi.org/10.1109/JPHOTOV.2013.2270351

[24] Mahmood, A., 'Recent research progress on quasi-solid-state electrolytes for dye-sensitized solar cells', *Journal of energy chemistry*, vol. 24, no. 6, pp. 686-692, 2015. https://doi.org/10.1016/j.jechem.2015.10.018

[25] Shi, L.-Y., Chen, T.-L., Chen, C.-H., Cho, K.-C., "Synthesis and characterization of a gel-type electrolyte with ionic liquid added for dye-sensitized solar cells. *International Journal of Photoenergy*", vol. 2013, pp. 1–7, 2013. (special issue) https://doi.org/10.1155/2013/834184

[26] An, H., Xue, B., Li, D., Li, H., Meng, Q., Guo, L., et al., "Environmentally friendly LiI/ethanol-based gel electrolyte for dye-

sensitized solar cells", *Electrochemistry Communications*, vol. 8, no. 1 pp. 170-172, 2006. https://doi.org/10.1016/j.elecom.2005.11.012

[27] Pathak, C., Surana, K., Kumar Shukla, V., & Singh, P. K., "Fabrication and characterization of a dye-sensitized solar cell using natural dyes", *Materials Today: Proceedings*, vol. 12, no. 3, pp. 665–670, 2019. https://doi.org/10.1016/j.matpr.2019.03.111

[28] Trihutomo, P., Soeparman, S., Widhiyanuriyawan, D., & Yuliati, L, "Performance Improvement of Dye-Sensitized Solar Cell- (DSSC-) Based Natural Dyes by Clathrin Protein", *International Journal of Photoenergy*, vol. 2019, pp. 1-9, 2019. (Article ID 4384728)

[29] Zanatta, Antonio Ricardo. "A fast-reliable methodology to estimate the concentration of rutile or anatase phases of TiO2." AIP Advances 7, no. 7 (2017): 075201.

[30] Shaikh, Shoyebmohamad F., Rajaram S. Mane, Byoung Koun Min, Yun Jeong Hwang, and Oh-shim Joo. "D-sorbitol-induced phase control of TiO2 nanoparticles and its application for dye-sensitized solar cells." Scientific reports 6, no. 1 (2016): 1-10.

[31] Zhuo, R. F., H. T. Feng, Q. Liang, J. Z. Liu, J. T. Chen, D. Yan, J. J. Feng et al. "Morphology-controlled synthesis, growth mechanism, optical and microwave absorption properties of ZnO nanocombs." Journal of Physics D: Applied Physics 41, no. 18 (2008): 185405.

[32] Umale, S. V., Tambat, S. N., Sudhakar, V., Sontakke, S. M., & Krishnamoorthy, K., "Fabrication, characterization, and comparison of DSSC using anatase TiO2 synthesized by various methods", *Advanced Powder Technology*, vol. 28, no. 11, pp. 2859–2864, 2017. https://doi.org/10.1016/j.apt.2017.08.012

[33] Wang, Q., Moser, J.-E., Grätzel, M., "Electrochemical impedance spectroscopic analysis of dye-sensitized solar cells", *The Journal of Physical Chemistry B*, vol. 109, no. 31, pp. 14945-14953, 2005. https://doi.org/10.1021/jp052768h

[34] Sarker, S., Ahammad, A., Seo, H. W., Kim, D. M., "Electrochemical impedance spectra of dye-sensitized solar cells: fundamentals and spreadsheet calculation", *International Journal of Photoenergy*, Vol. 2014, pp. 1-17, 2014. (Article ID 851705) https://doi.org/10.1155/2014/851705

[35] Fabregat-Santiago F, Bisquert J, Palomares E, Otero L, Kuang D, Zakeeruddin SM, Grätzel M., "Correlation between photovoltaic performance and impedance spectroscopy of dye-sensitized solar cells based on ionic liquids", *The Journal of Physical Chemistry C*, vol. 111, no. 17, pp. 6550-60, 2007. https://doi.org/10.1021/jp066178a

[36] Won, L.J., Kim, J.H. and Thogiti, S., 2018. A polymer electrolyte for dye-sensitized solar cells based on a poly (polyvinylidenefluoride-co-hexafluoropropylene)/hydroxypropyl methyl cellulose blend. Electronic Materials Letters, 14(3), pp.342-347. https://doi.org/10.1007/s13391-018-0031-4

[37] Dong, R.X., Shen, S.Y., Chen, H.W., Wang, C.C., Shih, P.T., Liu, C.T., Vittal, R., Lin, J.J. and Ho, K.C., 2013. A novel polymer gel electrolyte for highly efficient dye-sensitized solar cells. Journal of materials chemistry A, 1(29), pp.8471-8478. https://doi.org/10.1039/C3TA11331K

[38] Sonai, G. G., Tiihonen, A., Miettunen, K., Lund, P. D., & Nogueira, A. F., "Long-Term Stability of Dye-Sensitized Solar Cells Assembled with Cobalt Polymer Gel Electrolyte", *The Journal of Physical Chemistry C*, vol. 121, no. 33, pp.17577–17585.

This page is intentionally left blank